APPLICATIONS OF
MODELLING AND SIMULATION
http://arqiipubl.com/ams eISSN 2600-8084 VOL 3, NO. 1, 2019, 28-38

Prediction of Erosion Rate in Elbows for Liquid-Solid Flow via Computational Fluid Dynamics (CFD)

M. A. H. Yusof[1], Z. Zakaria[2], A. Supee[1,3*], M. Z. M. Yusop[4] and N. B. Haladin[5]

[1]School of Chemical and Energy Engineering, Faculty of Engineering, Universiti Teknologi Malaysia, Malaysia.
[2]Faculty of Engineering, Universiti Malaysia Sabah, Malaysia.
[3]Energy Management Group, School of Chemical and Energy Engineering, Faculty of Engineering, Universiti Teknologi Malaysia.
[4]School of Mechanical Engineering, Faculty of Engineering, Universiti Teknologi Malaysia, Malaysia.
[5]Language Academy, Universiti Teknologi Malaysia, Malaysia.

[*]Corresponding author: aizuddin@utm.my

Received 16 January 2019, Revised 15 February 2019, Accepted 16 February 2019.

Abstract: This paper predicts the effects of variety parameters such as particles size, stream velocities and elbows diameter on the erosion rate for an elbows in light crude oil-solid flow. A computational fluid dynamics (CFD) with commercially available FLUENT code (ANSYS 14.0) was applied to numerically predict erosion rate in elbows. Three separate models were used in CFD approach which are continuous flow modeling, Lagrangian particle tracking and empirical erosion equation. The ranges of parameters tested are 100-500 µm particles size, 3-7 m/s stream velocities and 0.0762-0.1778 m elbows diameter. From the results, maximum erosion rates increased with increasing size of particles and stream velocities and decreased with increasing elbows diameter. However, the location of the maximum erosion rate in elbows region was independent on those mentioned parameters.

Keywords: Computational fluid dynamics (CFD); Elbows diameter; Light crude oil-solid flow; Maximum erosion rate and location; Particles size and stream velocities.

1. INTRODUCTION

Fluids transportation with entrained solid particles or known as liquid-solid flow is a common process involved in the oil and gas industry. Normally, the fluids which are extracted from the reservoir and transported to the nearest processing plants or refineries will carry along the solid particles across the streamlines of the pipeline. The pipeline systems in practice do not consist an entirely straight length of pipe, but consists of entry length, elbows, valves, fittings as well as other fluids handling equipment such as pumps, compressors, heat exchangers, heaters, boilers and etc. When there are changes in fluids flow direction in the pipeline systems, the solid particle's inertia can cause it to deviate from streamlines of the carrying fluids, resulting in particles impingement on the wall of the components in pipeline systems. This phenomenon is referred to erosion because it involves metal removal process by solid particles impact [1-3]. The erosion damage may result in malfunction of the pipeline systems in a relatively short amount of time and caused in loss of productivity, expensive maintenance cost and a requirement to replace damaged components. Therefore, it is really important to minimise solid particles erosion effects as much as possible by having better understanding in the physics of particulate flow.

As part of the pipeline systems, elbows are vulnerable to erosive environment. Many researchers have selected elbows as their typical subject of erosion studies primarily because of its broad application and susceptibilities to erosion. Different approaching methods for erosion prediction in elbows were applied by them such as by experimental [4-6], empirical correlations and mechanistic models [7-10] and recently, the computational fluid dynamics (CFD) which has been widely used [11-14]. The effects of the particle rebound model on the particle trajectories as well as erosion pattern in the elbow and plugged tee was also investigated by Chen et al. [15] via both experimental and CFD approaches. They found that stream velocity affects the erosion rate and the maximum erosion rate occurred at the centre area of the elbow section due to the multiple impingements of one particle effects. Further results by them also shows that maximum erosion rate occurred almost at the centre area of the elbow section when they varied the diameter of the particles and elbows in the air flows [16]. However, different location of maximum erosion rate was observed when they replaced the air with the water flows. The location of the maximum erosion region shift to the exit region of the elbow. This is due to the high drag and inertia forces exerted on the particles by water. In addition, they concluded that for water/solid particles flow, the location of maximum erosion rate in the elbow is weakly influenced by flow parameters including stream velocity, elbows diameter and size of particles. These conclusions were also experimentally confirmed by previous researchers [17].

Erosion in elbows is a complex process and depends on a multitude factors such as the fluid and particles properties, production rate of produced fluid and particles, concentration of particles, diameter of elbows and particles size. Increase in stream velocity results in higher particles momentum produced and lead to the higher erosion rate [4,18-20]. Meanwhile, high particles volume concentration cause in erosion reduction in elbows due to the strong particle to particle interactions [11,16]. The severity of erosion decreased with increasing elbows diameter. This occurs since the impinging particles must pass through a larger stagnation region and thus allowing extra time for the particles to decelerate [21]. Smaller particles size results in less erosion [22-24] and different fluid types may cause in different erosion effects.

Due to the many involvement of elbows in pipeline systems, erosion prediction for this component is really significant. Despite a lot of research reported on the erosion prediction for the elbows component in pipeline [4-15], however, there is still lack of information on the prediction based on the stream velocity less than 10 m/s. In addition, present work uses different fluid type which is light crude oil ($C_{19}H_{30}$) as a liquid as compared to those reported works. In this research, CFD with commercially available FLUENT code (ANSYS 14.0) was applied to numerically predict erosion rate in elbows for a broad range of liquid/solid particles flow conditions. The elbows were tested under three different flow conditions named as stream velocity (3-7 m/s), size of sand particles (100-500 μm) and elbows diameter (0.0762-0.1778 m). Each flow conditions consist of five different sets of values and the results are presented in the form of maximum erosion rate graphs and visual illustration of erosion rate surface contours.

2. SIMULATION

The erosion prediction was performed in three separate models called as continuous flow modeling, particle tracking and application of empirical erosion equation. Continuous flow modeling was initiated by generating the computational grid and followed by specified solution options such as inlet and boundary conditions, turbulence model, and operating conditions. Particles were introduced into the flow after obtaining a flow solution at elbows. Lagrangian particles tracking approach was used to numerically determine the trajectories of droplets and solid particles through the flow field. The trajectory of particles were determined by considering the external forces acting on the particles. By using the information on particles impingement on the wall of elbows, the mass loss or erosion rate resulting from impingement was determined by empirical erosion equation. Table 1 listed all parameters and assumptions involved in CFD prediction modeling.

Table 1. Define parameters and assumptions in CFD simulator

<table>
<tr><th>Parameter</th><th>Description</th></tr>
<tr><td>Turbulence modelling</td><td>• Standard k-epsilon model</td></tr>
<tr><td>Fluid system</td><td>• Light crude oil ($C_{19}H_{30}$)
• Density (960 kg/m^3)
• Viscosity (0.048 kg/m.s)</td></tr>
<tr><td>Elbows system</td><td>• Material (carbon steel)
• Constant curvature ratio (1.5)
• 90° elbows</td></tr>
<tr><td>Operating temperature</td><td>• Room temperature (25 °C)</td></tr>
<tr><td>Particles system</td><td>• Material (sand)
• Number of particles (10000)
• Shape (spherical)
• Density (2600 kg/m^3) [4,11,25]</td></tr>
<tr><td>Assumptions</td><td>• The flow in the elbows are turbulence flow
• Incompressible and constant properties of fluid
• Spherical shape of particles in the particle tracking approach
• Constant radius curvature of elbows ($R/D = 1.5$)
• Interaction between solid particles and the effect of particles motion on the fluid flow are small and can be neglected</td></tr>
<tr><td>Tested flow conditions</td><td>
<table>
<tr><th>Flow conditions</th><th>Manipulated parameters</th><th>Stream (fluid and particles) velocity (m/s)</th><th>Elbows diameter (m)</th><th>Size of particles (μm)</th></tr>
<tr><td>1</td><td>Size of particles (μm) - 100, 200, 300, 400, 500</td><td>4</td><td>0.1016</td><td>-</td></tr>
<tr><td>2</td><td>Stream velocity (m/s) - 3, 4, 5, 6, 7</td><td>-</td><td>0.1016</td><td>200</td></tr>
<tr><td>3</td><td>Elbows diameter (m) - 0.0762, 0.1016, 0.1270, 0.1524, 0.1778</td><td>4</td><td>-</td><td>200</td></tr>
</table>
</td></tr>
</table>

2.1 The Continuous Phase Model

The conservation equations for mass and momentum in addition to the equations representing the turbulence model were used to predict the flow pattern of the continuous flow phase. Descriptions of the symbols used in this paper are given in Appendix. The equations used are as follows [26]:

Mass conservation equation:

$$(\partial/\partial x_j)(\rho \bar{U}_j) = 0 \tag{1}$$

Momentum conservation equation:

$$(\partial/\partial x_j)\,(\rho \bar{U}_i \bar{U}_j) \;=\; -\,(\partial P/\partial x_i) \;+\; (\partial/\partial x_j)(\mu \partial \bar{U}_i/\partial x_j)(\partial/\partial x_j)(\rho \overline{u_i u_j}) \tag{2}$$

where P is the static pressure and the stress tensor $\rho \overline{u_i u_j}$ is given by

$$\rho \overline{u_i u_j} = \mu\,(\partial \bar{U}_i/\partial x_j \;+\; \partial \bar{U}_j/\partial x_j) - 2/3\,\rho k \delta_{ij} \tag{3}$$

The δ_{ij} is equal to 0 if $i \neq j$, equals to 1 if $i = j$ and effective viscosity, $\mu_{eff} = \mu_T + \mu$

where δ_{ij} is Kronecker delta and turbulence viscosity, μ_T is given by

$$\mu_T = \rho\, C_\mu (k^2/\varepsilon) \tag{4}$$

with $C_\mu = 0.0845$

Equation (4) was obtained by solving both turbulence modeling equations (Equations (5) and (6)). The kinetic energy of turbulence:

$$(\partial/\partial x_j)(\rho \bar{U}_j k) \;=\; (\partial/\partial x_j)\,(\mu_{eff}/\sigma_k \;-\; \partial k/\partial x_j) \;+\; G_k \;-\; \rho\varepsilon \tag{5}$$

The dissipation rate of kinetic energy in turbulence:

$$(\partial/\partial x_j)\,(\rho \bar{U}_j \varepsilon) \;=\; (\partial/\partial x_i)\,(\mu_{eff}\;\partial\varepsilon\;/\sigma_\varepsilon\;\partial x_i) \;+\; C_{\varepsilon 1} G_k(\varepsilon/k) - (C_{\varepsilon 2} \;-\; C_{\varepsilon 3})\rho(\varepsilon^2/k) \tag{6}$$

where G_k represents the generation of turbulent kinetic energy due to the mean velocity gradients and it is given by

$$G_k = -\,\rho u_i u_j\,(\partial u_j/\partial x_i) \tag{7}$$

The quantities of σ_k and σ_ε are the effective Prandtl numbers for k and ε respectively and $C_{\varepsilon 3}$ as a function of the k/ε are given by previous researchers [27]. The model values for $C_{\varepsilon 1}$ and $C_{\varepsilon 2}$ are 1.42 and 1.68.

2.2 Particle Tracking

Basically, previous researchers use Eulerian and Lagrangian approaches to numerically determine the trajectories of droplets and solid particles through the flow field [28-30]. Durst et al. [28] compared both approaches in predicting particulate two phase flows and concluded that the Lagrangian approach has some distinct advantages for predicting the particulate flows with large acceleration. In addition, it could also handle particulate two phase flows consisting of poly dispersed particle size distribution. In this research, Lagrangian particles tracking approach has been selected in determining the velocity of the particles as well as its trajectory before any impact towards elbows wall. Solid surface erosion and determination of particle trajectory during the motion of following impact have been calculated by using this impact velocity data. Based on Newton's second law, governing equations of particles motion proposed by Clift et al. [31] have been applied in this research and it is described as follow:

$$m_p\,(dV_p/dt) \;=\; F_D \;+\; F_P \;+\; F_B \;+\; F_A \tag{8}$$

The above equation consists of drag force, pressure gradient force, buoyancy force and added mass force:

- Drag force $(F_D) \;=\; C_D \rho_f\, \pi\, \phi_p^2 |V_f - V_p|(V_f - V_p)/8$ (9)

where C_D is the drag coefficient and it is given by

$$C_D \;=\; (24/Re_s)\,(1 + 0.15 Re_s^{0.687}) \tag{10}$$

and particle relative Reynold number Re_s is defined by

$$Re_s = [\rho_f |V_p - V_f| \phi_p]/\mu_f \quad (11)$$

- Pressure gradient force $(F_P) = \pi \phi_p^3 \ \nabla P/4$ (12)
- Buoyancy force $(F_B) = \pi \phi_p^3(\rho_p - \rho_f)g/6$ (13)
- Added mass force $(F_A) = -(\pi \phi_p^3 \rho_p dV_p)/12dt$ (14)

2.3 Erosion Rate (*ER*) Prediction

The model available in the FLUENT code for the calculation of the *ER* has been selected by taking into consideration the parameters such as mass flow rate of the particles $(\dot{m}_p)$, function of particles diameter $(C(\phi_p))$, function of the impact angle $(f(\alpha))$, relative particles velocity (V_p), function of relative particles velocity $(b(V_p))$ and the area of the wall face where the particles strikes the boundary (A_{face}). The empirical erosion equation used is as follows:

$$ER = \sum_{i=1}^{Nparticle} \dot{m}_p C(\phi_p) f(\alpha) V_p^{b(Vp)} / A_{face} \quad (15)$$

3. RESULTS AND DISCUSSION

Three parameters were changed to demonstrate their influence on erosion rate of the elbows component. The three parameters were size of particles (100-500 µm), stream velocity (3-7 m/s) and elbows diameter (0.0762-0.1778 m). The Reynolds number was range from 4572 to 24892. During the simulation, another two parameters were kept constant for each tested flow conditions as mentioned in Table 1. The effects of flow conditions viz. size of particles, stream velocity and elbows diameter on erosion rate of the elbows component are presented in the form of maximum erosion rate graphs and visual illustration of erosion rate surface contours.

3.1 Effects of Particles Size Towards Elbows (Erosion Rate at Flow Condition 1)

Erosion rate surface contours for the particles diameter ranging from 100 to 500 µm are depicted in Figure 1 to Figure 5. Overall, there is no specific trend for the location of maximum erosion rate when the size of particles varied. Particles size of 100 µm, 300 µm, 400 µm and 500 µm show maximum erosion rate occurred towards exit region of the elbows. Meanwhile for 200 µm, there are two locations of maximum erosion rate observed and it is located almost at the centre area of the elbow section and towards exit region of the elbows. No specific trend in the location of maximum erosion rate shows similarity with previous works conducted [16-17]. The possible explanation for the similarity might be due to the density of carrier fluid used. Only slightly different in value between the density of water (997 kg/m^3) and light crude oil (960 kg/m^3) at 25 °C. Thus, the drag force exerted on particles by carrier fluid more less have the same magnitude for both water and light crude oil system. In addition, particle with 100 µm indicates clear impingement at the inlet section of elbows compared to other size of particles. This might be due to the smaller size of particles which is lightweight and easier to deviate from streamline at the entrance region of the elbow. After multiple impingements at the entrance region of the elbow, the deviated particles then follow the streamline again and strikes the exit region of the elbow.

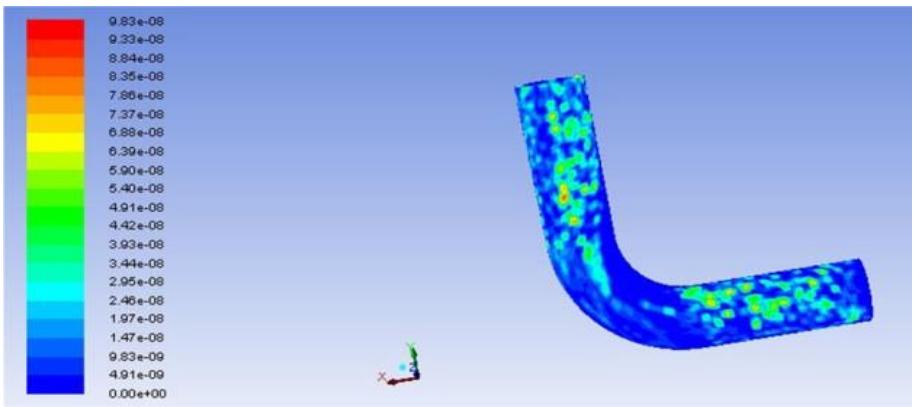

Figure 1. Erosion rate surface contour (kg/m^2.s) for 100 µm particles size

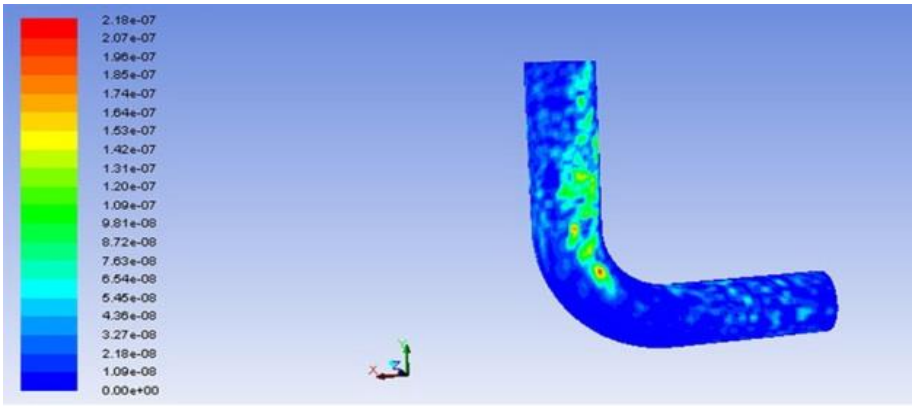

Figure 2. Erosion rate surface contour (kg/m^2.s) for 200 µm particles size

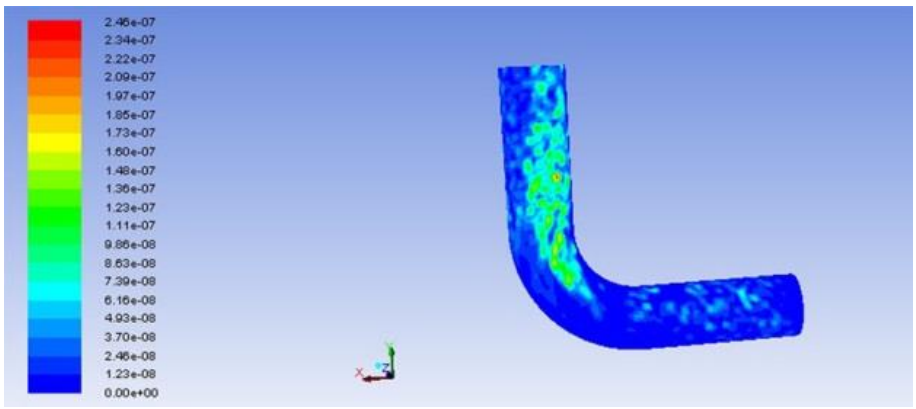

Figure 3. Erosion rate surface contour (kg/m^2.s) for 300 µm particles size

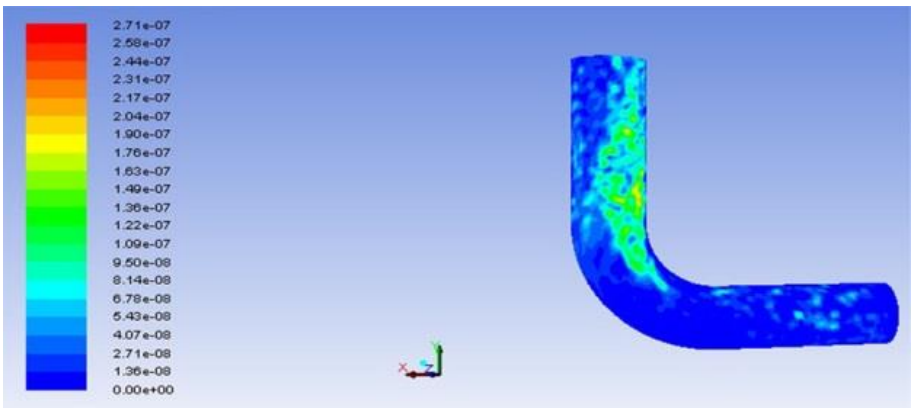

Figure 4. Erosion rate surface contour (kg/m^2.s) for 400 µm particles size

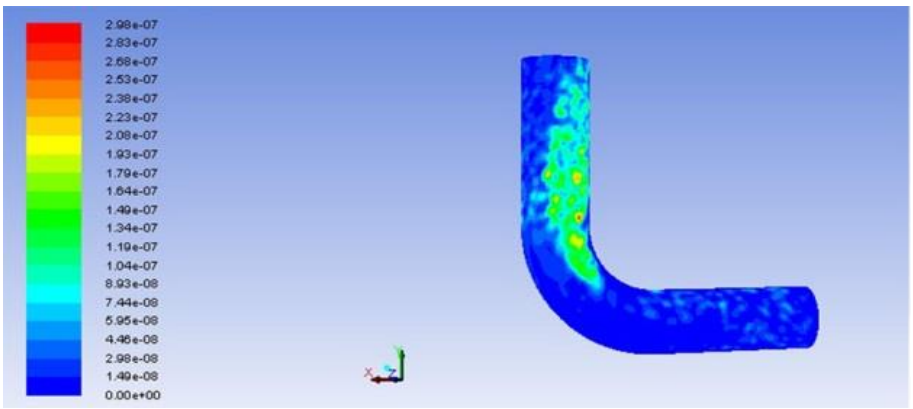

Figure 5. Erosion rate surface contour (kg/m^2.s) for 500 µm particles size

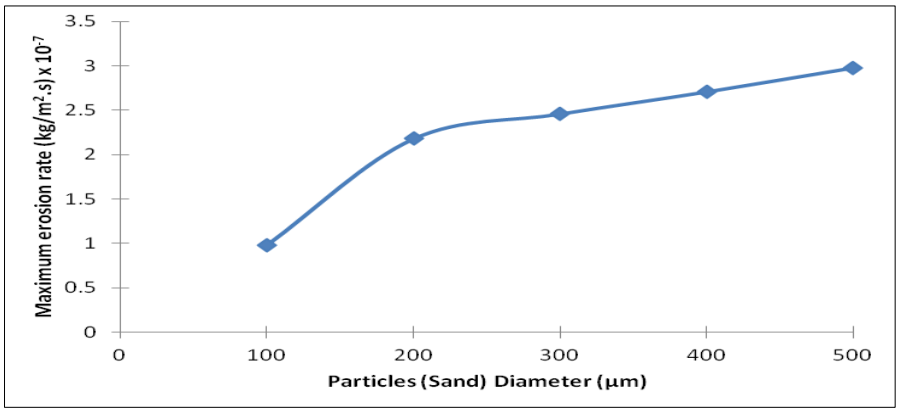

Figure 6. Maximum erosion rate (kg/m^2.s) × 10^{-7} for various particles diameter (µm)

Figure 6 shows maximum erosion rate occurred for the elbow with flow condition 1. Maximum erosion rate was affected by the size of particles and increased in particles size will lead to the increased in maximum erosion rate. Particle size of 500 µm results in the highest maximum erosion rate which is 2.98 × 10^{-7} kg/m^2.s. Larger particles size leads to higher kinetic energy and therefore, results in larger or deeper indentations on the wall of elbows. The larger or deeper indentation, the greater the amount of material removed or in another word, the higher maximum erosion rate. However, there is a limitation to the size of the larger particles of which they tend to move slowly or settle the carrying fluid and therefore they are not likely to cause severe erosion. For this research, only particles size range from 100 to 500 µm were selected since it is common size found in oil and gas industry [25].

3.2 Effects of Stream Velocity Towards Elbows (Erosion Rate at Flow Condition 2)

Figure 7 to Figure 11 illustrate erosion rate surface contours for the tested elbows at different stream velocities. All the velocities show similarity in term of the location of the maximum erosion rate which occurred towards exit region of the elbows. This probably due to the gravity effects as the flow moves in upward direction of the elbow. In horizontal area of the elbow (inlet to near the centre), the gravity effects are negligible. In vertical area of the elbow (exit region), the flow against the gravity direction and as a consequences, the particles tends to impinge at the exit region of the elbow. Increased in stream velocity causes in increase in erosion severity. At high stream velocity, the momentum and inertia of the particles and fluid will increase and as a consequences, the collision between particles and the wall of the elbows also will increase. This is the reason why stream velocity of 7 m/s as shown in Figure 11 results in severe erosion rate surface contours compared to other stream velocities.

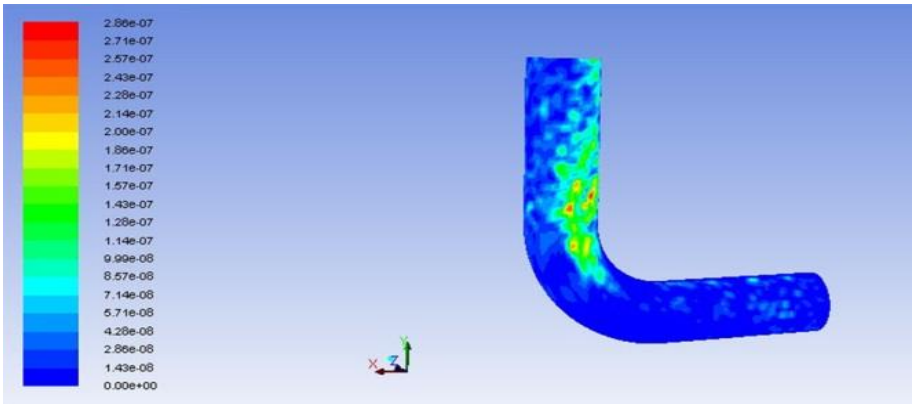

Figure 7. Erosion rate surface contour (kg/m^2.s) for 3 m/s stream velocity

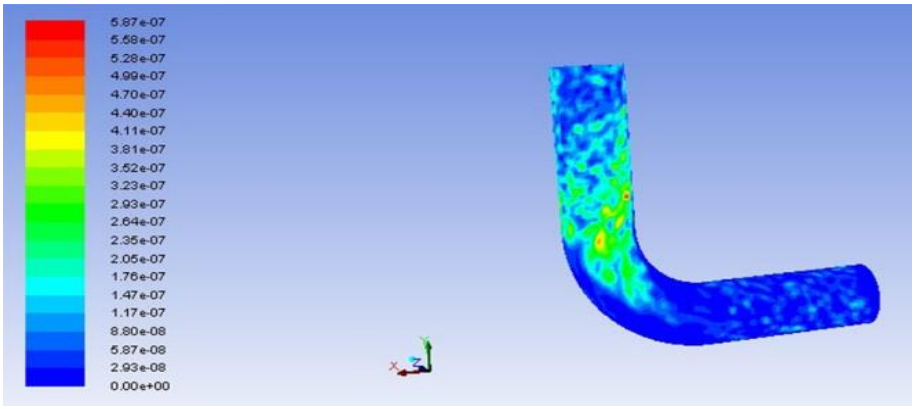

Figure 8. Erosion rate surface contour (kg/m^2.s) for 4 m/s stream velocity

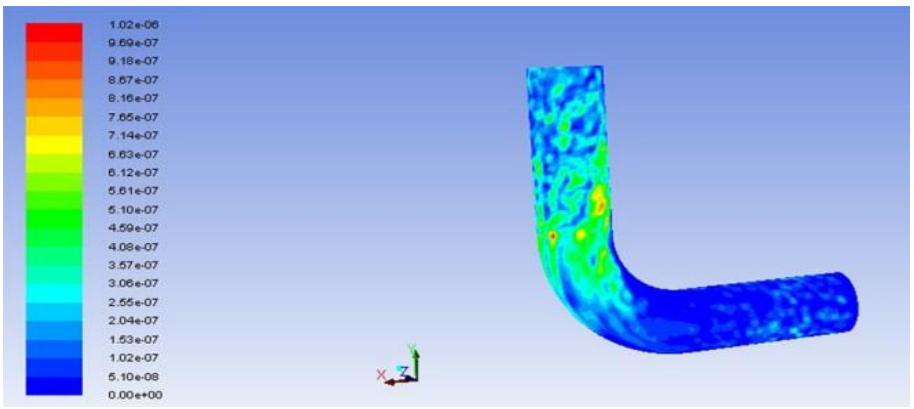

Figure 9. Erosion rate surface contour (kg/m^2.s) for 5 m/s stream velocity

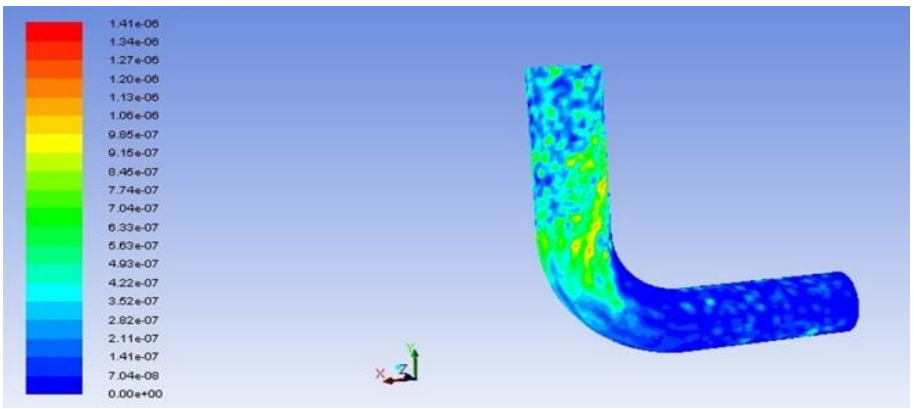

Figure 10. Erosion rate surface contour (kg/m^2.s) for 6 m/s stream velocity

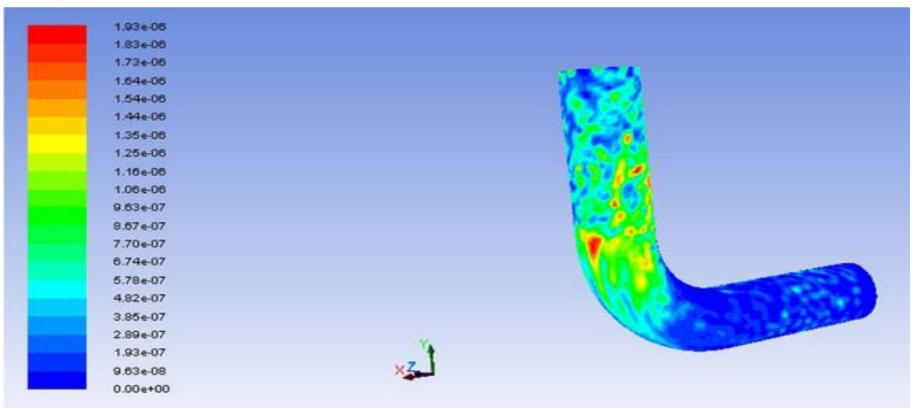

Figure 11. Erosion rate surface contour (kg/m^2.s) for 7 m/s stream velocity

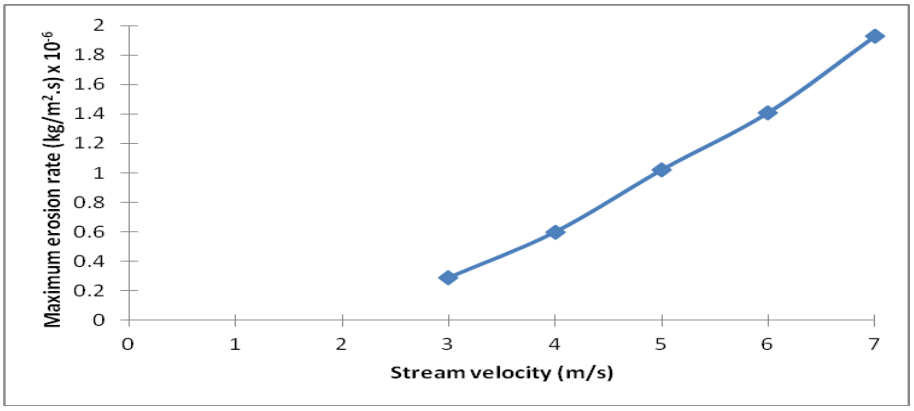

Figure 12. Maximum erosion rate (kg/m^2.s) for various stream velocity (m/s)

Further illustration on the severity values of the erosion rate due to the stream velocities is depicted in Figure 12. Maximum erosion rate was increased from 0.286 × 10^{-6} kg/m^2.s to 1.93 × 10^{-6} kg/m^2.s when the stream velocity change from 3 m/s to 7 m/s. The trend obtained also shows a similar pattern with previous works done [15,21,26,32-33].

3.3 Effects of Elbows Diameter Towards Elbows (Erosion Rate at Flow Condition 3)

Erosion rate surface contours for five different size of elbows are shown in Figure 13 to Figure 17. Similar patterns produced as the effects of stream velocity where maximum erosion rate occurred towards exit region of the elbows component. The plot of maximum erosion rate versus elbows diameter is depicted in Figure 18. Smaller elbow diameter will cause in higher maximum erosion rate and the trend reverses when bigger elbows diameter were used. As the elbow diameter increases, the particles must pass through more fluid before impinging the wall. In other words, the stagnation length increases with increasing elbows diameter. Therefore, the fluid has a greater chance to decelerate the particles approaching the wall of elbow. This leads to a decrease in maximum erosion rate with an increase in elbows diameter. It was found that the stagnancy length dependency on the elbow diameter larger than 0.1524 m is weak [1]. This possibly contributes to the insignificant changes in maximum erosion rate exceeding 0.1524 m as depicted in Figure 18.

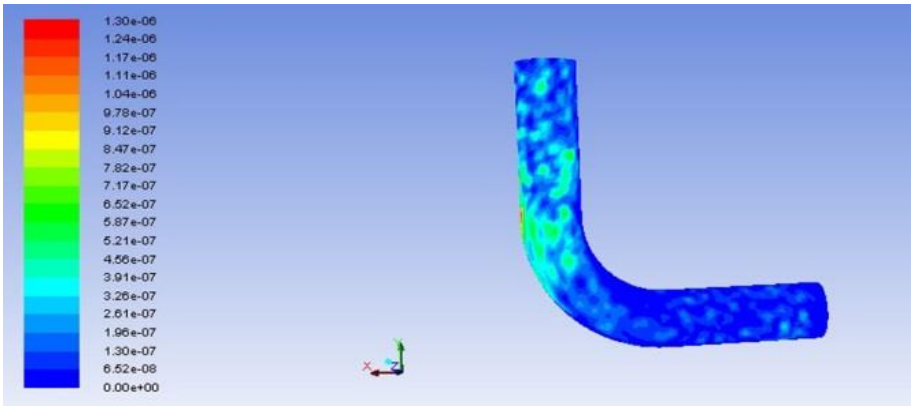

Figure 13. Erosion rate surface contour (kg/m^2.s) for 0.0762 m elbows diameter

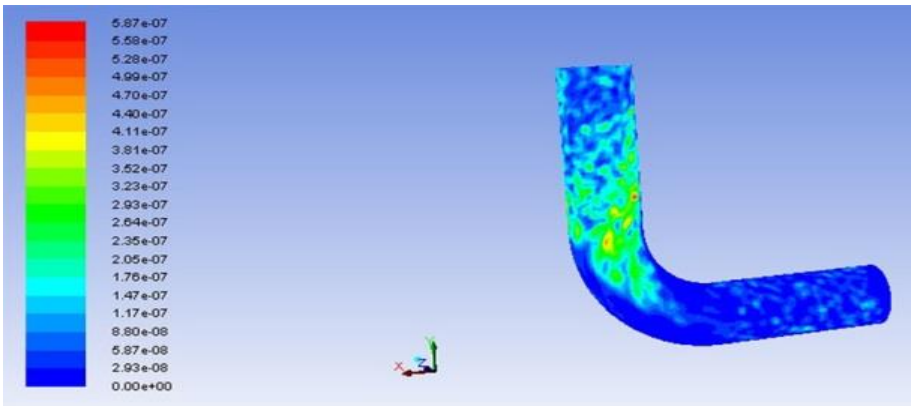

Figure 14. Erosion rate surface contour (kg/m^2.s) for 0.1016 m elbows diameter

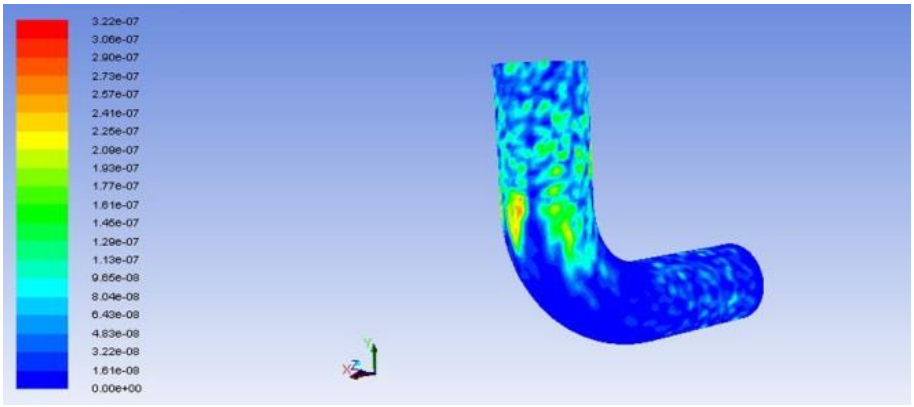

Figure 15. Erosion rate surface contour (kg/m^2.s) for 0.1270 m elbows diameter

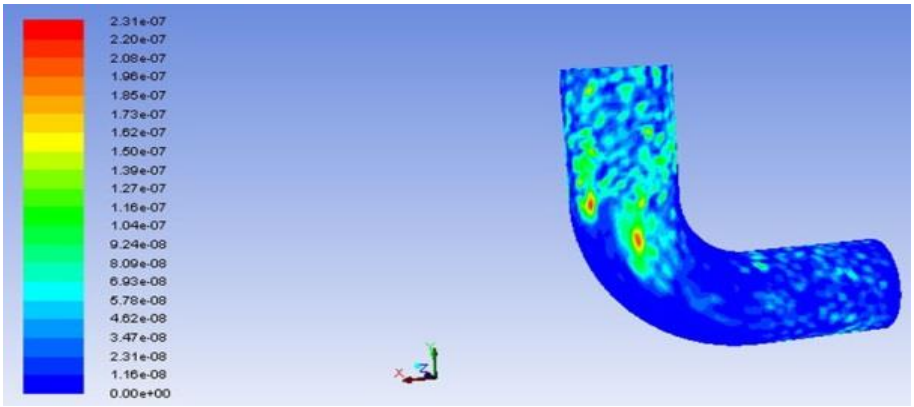

Figure 16. Erosion rate surface contour (kg/m^2.s) for 0.1524 m elbows diameter

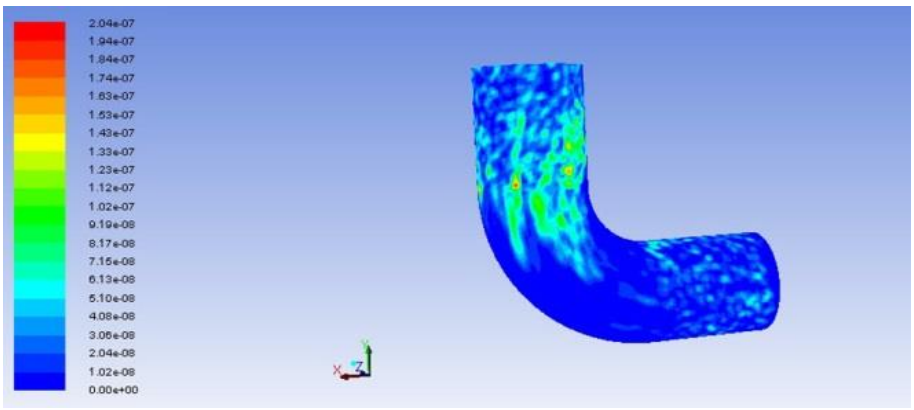

Figure 17. Erosion rate surface contour (kg/m^2.s) for 0.1778 m elbows diameter

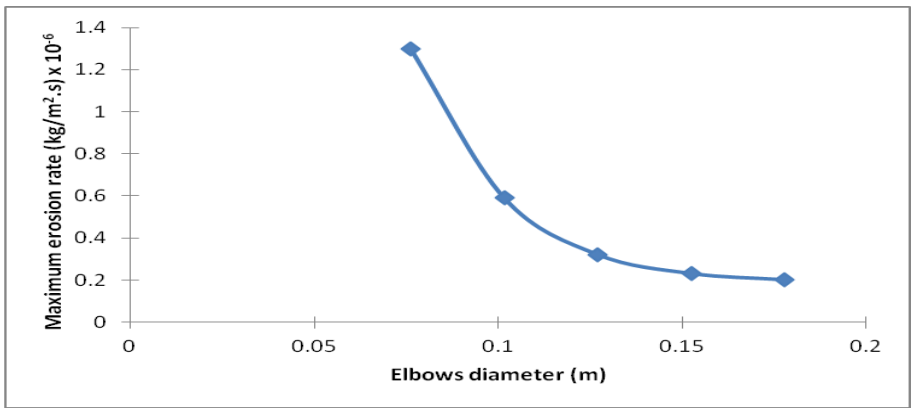

Figure 18. Maximum erosion rate (kg/m^2.s) for various elbows diameter (m)

4. CONCLUSION

The following conclusions are drawn from the analyses:

1. The location of maximum erosion rate in the elbow is weakly influenced by flow parameters including stream velocity, elbows diameter and size of particles.
2. Larger stagnation region produced by bigger elbows diameter provide opportunities for the particles to decelerate due to the longer travel time in fluids before they reach the wall of elbows.
3. Particles size and stream velocity are directly proportional to the maximum erosion rate. Higher velocity results in rapid collision between particles and the wall of the elbows and bigger particles size will cause in deeper indentations on the wall of elbows. As a consequence, higher maximum erosion rate will be produced.

The simulation results could possibly assist in design process for the real field which has the same condition and parameters. By having a proper design, the cost of maintenance in terms of elbow replacement due to the erosion could be reduced.

ACKNOWLEDGEMENT

The Department of Energy Engineering, School of Chemical and Energy Engineering and UTM are highly acknowledged for providing continuous technical and facilities support.

REFERENCES

[1] M. Parsi, K. Najmi, F. Najafifard, S. Hassani, B. S. McLaury and S. A. Shirazi, A comprehensive review of solid particle erosion modeling for oil and gas wells and pipelines applications, *Journal of Natural Gas Science and Engineering*, 21, 850–873, 2014.

[2] G. Ou, K. Bie, Z. Zheng, G. Shu, C. Wang and B. Cheng, Numerical simulation on the erosion wear of a multiphase flow pipeline, *The International Journal of Advanced Manufacturing Technology*, 96, 1705–1713, 2018.

[3] A. Mansouri, *A combined CFD-experimental method for developing an erosion equation for both gas-sand and liquid-sand flows*, Ph.D. Dissertation, The University of Tulsa, 2016.

[4] R. E. Vieira, A. Mansouri, B. S. McLaury and S. A. Shirazi, Experimental and computational study of erosion in elbows due to sand particles in air flow, *Powder Technology*, 288, 339–353, 2016.

[5] A. Asgharpour, P. Zahedi, H. A. Khanouki, S. A. Shirazi and B. S. McLaury, Experimental and numerical study on solid particle erosion in elbows mounted in series, *Proceedings of the ASME 2017 Fluids Engineering Division Summer meeting*, Hawaii, USA, 2017, pp. 1–11.

[6] A. Mansouri, H. Arabnejad, S. Karimi, S. A. Shirazi and B. S. McLaury, Improved CFD modeling and validation of erosion damage due to fine sand particles, *Wear*, 338–339, 339–350, 2015.

[7] P. Zahedi, S. Parvandeh, A. Asgharpour, B. S. McLaury, S. A. Shirazi and B. A. McKinney, Random forest regression prediction of solid particle erosion in elbows, *Powder Technology*, 338, 983–992, 2018.

[8] M. Parsi, H. Arabnejad, A. Al-Sarkhi, P. Zahedi, R. E. Vieira, P. Sharma and B. S. McLaury, A new correlation for predicting solid particle erosion caused by gas-sand flow in elbows, *Offshore Technology Conference*, Texas, USA, 2018, pp. 1–18.

[9] R. Kang and H. Liu, A mechanistic model of predicting solid particle erosion on the symmetry plane of elbows for annular flow, *Journal of Energy Resources Technology*, 141, 032907, 2019.

[10] H. Liu, W. Yang and R. Kang, A correlation for sand erosion prediction in annular flow considering the effect of liquid dynamic viscosity, *Wear*, 404, 1–11, 2018.

[11] C. A. R. Duarte, F. J. de Souza and V. F. dos Santos, Numerical investigation of mass loading effects on elbow erosion, *Powder Technology*, 283, 593–606, 2015.

[12] J. Chen, Y. Wang, X. Li, R. He, S. Han and Y. Chen, Erosion prediction of liquid-particle two-phase flow in pipeline elbows via CFD–DEM coupling method, *Powder Technology*, 275, 182–187, 2015.

[13] C. Li, Q. Huang, S. Yan and T. Huang, Parametric CFD studies on erosion in 3D double elbow, *International Journal of Engineering Systems Modelling and Simulation*, 8, 264–272, 2016.

[14] T. A. Sedrez, Y. R. Rajkumar, S. A. Shirazi, K. Sambath and H. J. Subramani, CFD simulations and experiments of sand erosion for liquid dominated multiphase flows in an elbow, *11th North American Conference on Multiphase Production Technology*, Banff, Canada, 2018, pp. 1–12.

[15] X. Chen, B. S. McLaury and S. A. Shirazi, Application and experimental validation of a computational fluid dynamics (CFD)-based erosion prediction model in elbows and plugged tees, *Computers & Fluids*, 33, 1251–1272, 2004.

[16] X. Chen, B. S. McLaury and S. A. Shirazi, Numerical and experimental investigation of the relative erosion severity between plugged tees and elbows in dilute gas/solid two-phase flow, *Wear*, 261, 715–729, 2006.

[17] D. J. Blanchard, P. Griffith and E. Rabinowicz, Erosion of a pipe bend by solid particles entrained in water, *Journal of Engineering for Industry*, 106, 213–217, 1984.

[18] R. Verma, V. K. Agarwal, R. K. Pandey and P. Gupta, Erosive wear reduction for safe and reliable pneumatic conveying systems: review and future directions, *Life Cycle Reliability and Safety Engineering*, 7, 193–214, 2018.

[19] S. Shamshirband, A. Malvandi, A. Karimipour, M. Goodarzi, M. Afrand, D. Petković, M. Dahari and N. Mahmoodian, Performance investigation of micro-and nano-sized particle erosion in a 90 elbow using an ANFIS model, *Powder Technology*, 284, 336–343, 2015.

[20] H. H. Ya, M. F. Othman, W. Pao, N. N. Tran and R. Khan, Simulation study on impact of fine sand particle to 90° steel elbow in pipe, *AIP Conference Proceedings*, 2035, 030003, 2018.
[21] B. S. McLaury, J. Wang, S. A. Shirazi, J. R. Shadley and E. F. Rybicki, Solid particle erosion in long radius elbows and straight pipes, SPE Annual Technical Conference and Exhibition, San Antonio, Texas, 1997, pp. 977–986.
[22] V. B. Nguyen, Q. B. Nguyen, Y. W. Zhang, C. Y. H. Lim and B. C. Khoo, Effect of particle size on erosion characteristics, *Wear*, 348-349, 126–137, 2016.
[23] J. Pei, A. Lui, Q. Zhang, T. Xiong, P. Jiang and W. Wei, Numerical investigation of the maximum erosion zone in elbows for liquid-particle flow, *Powder Technology*, 333, 47–59, 2018.
[24] W. S. Khur and Y. Y. Jian, CFD study of sand erosion in pipeline, *Journal of Petroleum Science and Engineering*, 176, 269–278, 2019.
[25] N. A. Barton, *Erosion in elbows in hydrocarbon production systems: Review document*, Glasgow, 2003.
[26] M. A. Habib, H. M. Badr, R. Ben-Mansour and M. E. Kabir, Erosion rate correlations of a pipe protruded in an abrupt pipe contraction, *International Journal of Impact Engineering*, 34, 1350–1369, 2007.
[27] T.-H. Shih, W. W. Liou, A. Shabbir, Z. Yang and J. Zhu, A new k-ϵ eddy viscosity model for high reynolds number turbulent flows, *Computers & Fluids*, 24, 227–238, 1995.
[28] F. Durst, D. Miloievic and B. Schönung, Eulerian and lagrangian predictions of particulate two-phase flows: a numerical study, *Applied Mathematical Modelling*, 8, 101–115, 1984.
[29] A. Picart, A. Berlemont and G. Gouesbet, Modelling and predicting turbulence fields and the dispersion of discrete particles transported by turbulent flows, *International Journal of Multiphase Flow*, 12, 237–261, 1986.
[30] Q. Q. Lu, J. R. Fontaine and G. Aubertin, A lagrangian model for solid particles in turbulent flows, *International Journal of Multiphase Flow*, 19, 347–367, 1993.
[31] R. Clift, J. R. Grace and M. E. Weber, *Bubbles, Drops, and Particles*, New York, 1978.
[32] A. T. Bourgoyne Jr., Experimental study of erosion in diverter systems due to sand production, SPE/IADC Drilling Conference, New Orleans, Louisiana, 1989, pp. 807–816.
[33] B. S. McLaury, E. F. Rybicki, J. R. Shadley and S. A. Shirazi, How operating and environmental conditions affect erosion, CORROSION, San Antonio, Texas, 1999, pp. 1–24.

APPENDIX

Nomenclature		**Greek symbols**	
x	space coordinate	ρ	density
$\bar{U}$	time average velocity component	μ	viscosity
P	pressure	δ_{ij}	Kronecker delta
u	fluctuating component of velocity	σ_k	effective Prandtl number for k
k	kinetic energy of turbulence	σ_ε	effective Prandtl number for ε
$C_\mu, C_{\varepsilon 1}, C_{\varepsilon 2}$	empirical constants in k-epsilon turbulence model	ε	rate of dissipation of the kinetic energy
G_k	production of turbulent kinetic energy due to mean velocity gradients	ϕ	diameter
F	force	$\dot{m}$	mass flow rate
m	mass	∂	partial derivative
V	velocity		
C_D	drag coefficient	**Subscripts**	
Re_s	particle relative Reynold number	i, j	spatial coordinate indices
t	time	eff	effective
g	gravity	T	turbulence
$\dot{m}$	mass flow rate	D	drag
ER	erosion rate	P	pressure gradient
$C(\phi)$	function of the diameter	B	buoyancy
$f(\alpha)$	function of the impact angle	A	added mass
V	relative velocity	t	time
A	area	f	fluid
d	derivative	p	particle
Superscripts		$face$	wall face where the particles strikes the boundary
$\overline{\quad}$	time average		
$\dot{}$	time rate		
$b(\mathrm{V})$	function of relative velocity		